Dispersion of Functionalized Carbon Nanotubes in Polystyrene

Cynthia A. Mitchell,[†] Jeffrey L. Bahr,[‡] Sivaram Arepalli,[§] James M. Tour,*[,‡] and Ramanan Krishnamoorti*[,†]

Department of Chemical Engineering, University of Houston, Houston, Texas 77204-4004; Department of Chemistry, Department of Mechanical Engineering and Materials Science, and Center for Nanoscale Science and Technology, Rice University, MS222, Houston, Texas 77005; and G. B. Tech./ NASA-Johnson Space Center, Houston, Texas 77058

Received June 10, 2002

ABSTRACT: Polystyrene nanocomposites with functionalized single-walled carbon nanotubes (SWNTs), prepared by the in-situ generation and reaction of organic diazonium compounds, were characterized using melt-state linear dynamic viscoelastic measurements. These were contrasted to the properties of polystyrene composites prepared with unfunctionalized SWNTs at similar loadings. The functionalized nanocomposites demonstrated a percolated SWNT network structure at concentrations of 1 vol % SWNT, while the unfunctionalized SWNT-based composites at twice the loading of SWNT exhibited viscoelastic behavior comparable to that of the unfilled polymer. This formation of the SWNT network structure for the functionalized SWNT-based composites is because of the improved compatibility between the SWNTs and the polymer matrix and the resulting better dispersion of the SWNT.

Introduction

Development of single-walled carbon nanotube (SWNT)-based polymer nanocomposites has the potential for the tailoring of unique lightweight materials with distinctly superior mechanical, thermal, and electronic properties. The development of such composites has been impeded by the inability to disperse SWNTs, which typically appear as ropes, in the polymer matrix due to the lack of chemical compatibility between the polymers and the SWNTs.[1] A cursory summation of important areas for composites with SWNTs would include homogeneity of dispersion, interfacial compatibility with the matrix, and the exfoliation of SWNT ropes and bundles. Chemical modification of SWNTs, be it covalent or noncovalent, may help address all of these concerns by the attachment of appropriate moieties to the surface of SWNTs. The covalent chemistry of SWNTs has been reviewed,[2] and this area is actively being investigated. Using these techniques, one can envision attachment of moieties that both facilitate dispersion and provide for chemical bonding with the matrix. We demonstrate here the benefit of functionalized SWNTs by examination of melt-state rheology of polystyrene/SWNT composites.

We draw inspiration from previous work in layered silicates (smectites or nanoclays), where organic modification, by ion-exchange of the metal cations with organic cations, renders the pristine hydrophilic silicates to be hydrophobic or organophilic and capable of being intercalated or exfoliated by polymeric matrices.[3−5] Two theoretical arguments have been proposed to justify the incorporation of polymers between the silicate layers;[5−7] the simpler mean field theory of Vaia and Giannelis[7] suggests that the intercalation of polymers results almost entirely due to enthalpic interactions. They demonstrated, with experimental verification,[5] that even though the polymer had unfavorable interactions with the silicate, and the tail of the organic surfactant modifier had repulsive interactions with both the polymer and the silicate, intercalation was possible by simply ensuring that the polymer/silicate interaction was less unfavorable than the surfactant/silicate interaction. However, to obtain a truly exfoliated state, highly favorable interactions between the polymer and the silicate were necessary.

In the case of layered-silicate polymer composites, the state of mixing is conveniently probed directly using X-ray diffraction and electron microscopy, because of the layer−layer registry and the large electron density contrast between the silicate sheets and the polymer matrix.[4,8] On the other hand, for mixtures of SWNTs and polymers, the electron density contrast is poor, making the application of electron microscopy and X-ray diffraction slightly complicated. However, melt state rheology has proven to be a powerful mechanism to examine the superstructure of filled systems ranging from liquidlike dispersion of block copolymer micelles,[9] isotropic carbon black-filled elastomers,[10] steric stabilized silica particles[11] and layered silicate-based polymer nanocomposites.[12−15] We exploit the changes in the linear response to applied small-amplitude oscillatory strain from composites prepared with a model monodisperse polystyrene and functionalized and unfunctionalized SWNTs in order to elucidate the changes in dispersion.

Experimental Section

Methylene chloride and acetonitrile were distilled from calcium hydride. Dimethylformamide (DMF) was distilled and stored over molecular sieves. Tetrahydrofuran (THF) was distilled from sodium/benzophenone ketyl. Pyridine was distilled immediately prior to use. All other reagents were obtained commercially and used without further purification. Raman spectra were collected from solid samples, with excitation at 780 nm. UV/vis/NIR absorption spectra were collected in double-beam mode, with solvent reference. Solutions for these experiments were prepared with the aid of sonication. Homogenization was performed using a IKA UltraTurrax T25. TGA data were collected in an argon atmosphere, with a heating rate of 5 °C min^{-1}. Details of the synthesis and mixing and characterization of the nanocomposites are described below.

[†] University of Houston.
[‡] Rice University.
[§] G. B. Tech./NASA-Johnson Space Center.

10.1021/ma020890y CCC: $22.00
Published on Web 09/28/2002

4-(10-Hydroxydecyl)nitrobenzoate (1). In a 250 mL round-bottom flask, under nitrogen, a 42.26 g (242.2 mmol) portion of 1,10-dihydroxydecane was dissolved in 200 mL of distilled pyridine. This solution was then cooled with an ice bath, and a solution of 4-nitrobenzoyl chloride (15.00 g, 80.8 mmol) in 120 mL of dichloromethane was slowly added. After 1 h the ice bath was removed, and the solution was stirred for 15 h at room temperature. The solution was then diluted with 100 mL of dichloromethane and washed three times with 50 mL portions of water. The organic phase was dried over magnesium sulfate and then filtered, and the solvent was removed by distillation at reduced pressure. The residual oil was dissolved in hexanes:ethyl acetate (1:2) and chromatographed on silica, using hexanes:ethyl acetate (2:1) as the eluent. The product was isolated as a light-yellow oil that crystallized on standing (12.9 g, 50%). An additional portion of the title compound was collected as a mixture with a second product and was retained for future use; mp 62−66 °C. IR (KBr): 3302.2, 3201.2, 2931.2, 2905.4, 2863.3, 2849.2, 1728.9, 1524.9, 1354.5, 1284.1, 1130.4, 1104.13, 716.73 cm^{-1}. ^1H NMR (400 MHz, $CDCl_3$): δ 8.30 (d, J = 8.9 Hz, 2 H), 8.22 (d, J = 8.9 Hz, 2 H), 4.38 (t, J = 6.7 Hz, 2 H), 3.65 (t, J = 6.6 Hz, 2 H) 1.80 (quint, J = 6.8 Hz, 2 H) 1.58 (quint, J = 7.2 Hz, 2 H), 1.48 to 1.33 (m, 12 H). ^{13}C NMR (100 MHz, $CDCl_3$): 165.17, 150.89, 136.28, 131.06, 123.92, 66.50, 63.42, 33.17, 29.88, 29.81, 29.78, 29.61, 29.00, 26.35, 26.13. HRMS calculated for $C_{17}H_{25}NO_5$: 323.173 273. Found: 323.173 087.

4-(10-Hydroxydecyl)aminobenzoate (2). **1** (5.00 g, 15.5 mmol) was dissolved in 40 mL of absolute ethanol, and a catalytic amount of 10% Pd/C was added. The suspension was hydrogenated on a Parr apparatus (55 psi, 23 °C) for 20 min and then filtered through Celite, washing with ethanol. The solvent was removed by distillation at reduced pressure to give a clear oil that crystallized on standing (4.37 g, 96%); mp 76−78 °C. IR (KBr): 3500.8, 3338.9, 3221.7, 2926.7, 2851.6, 1687.7, 1640.7, 1603.2, 1519.7, 1278.1, 1166.8, 1126.7, 1045.7, 1008.37, 840.69, 772.18 cm^{-1}. ^1H NMR (400 MHz, $CDCl_3$): δ 7.86 (d, J = 8.6 Hz, 2 H), 6.66 (d, J = 8.6 Hz, 2 H), 4.26 (t, J = 6.7 Hz, 2 H), 3.64 (t, J = 6.6 Hz, 2 H), 1.74 (quint, J = 6.8 Hz, 2 H), 1.59 to 1.71 (m, 2 H), 1.45 to 1.32 (m, 12 H). ^{13}C NMR ($CDCl_3$): 167.23, 151.15, 131.95, 120.49, 114.23, 64.93, 63.42, 33.19, 29.89, 29.82, 29.78, 29.64, 29.19, 26.45, 26.12. HRMS calculated for $C_{17}H_{27}NO_3$: 293.199 094. Found: 293.198 914.

4-(10-Hydroxydecyl)benzoate−SWNT (3). SWNTs (940 mg) were homogenized in a mixture of 1.5 L of 1,2-dichlorobenzene and 300 mL of THF for a period of 20 min. The suspension was transferred to a 2 L round-bottom flask equipped with a magnetic stir bar and a thermometer. The solution was sparged with nitrogen for 20 min, and **2** (34.50 g, 117.5 mmol) was then added all at once. The flask was sealed with a rubber septum and then evacuated and backfilled with nitrogen. Isoamyl nitrite (18.30 g, 156.6 mmol) was added by syringe. The contents were heated and stirred at an internal temperature of 55−60 °C for 48 h. Upon cooling of the reaction mixture, the suspension was diluted with 100 mL of DMF and then filtered to a wet cake over a PTFE membrane (0.45 μM). The cake was washed with an additional 50 mL portion of DMF, then transferred to an Erlenmeyer flask containing 200 mL of DMF, and homogenized for 20 min. The suspension was again filtered to a wet cake, washed with 25 mL of DMF, and again subjected to homogenization in DMF. After a final filtration (the filtrate was clear at this point), the cake was washed with 40 mL of ethyl acetate and kept wet. The wet cake was spread out on a glass plate and dried under vacuum (ca. 0.8 mmHg) at 55 °C for 15 h. The fluffy resulting material was scraped off the glass plate to obtain a total of 1.20 g. Residual mass on heating to 800 °C in argon: 74.2%. The organic content indicates that on an average one out of every 66 C in the SWNT is functionalized.

Polymer. The polymer used in this study was a model anionically polymerized atactic polystyrene obtained from Polymer Source and was used as obtained. The molecular weight was determined by gel permeation chromatography; the weight-average molecular weight (M_w) was 152 000 Da with a polydispersity ratio (M_w/M_n) of <1.05.

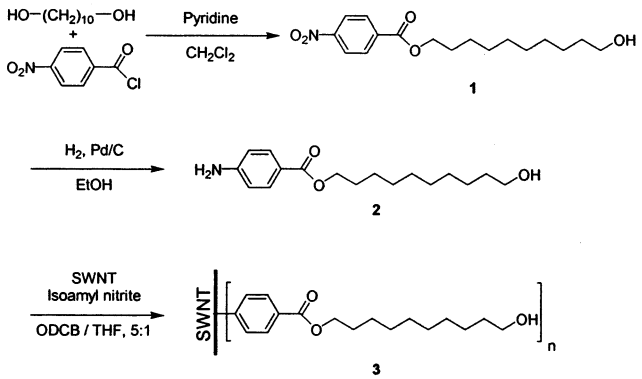

Figure 1. Preparation of functionalized SWNT material and the requisite precursors.

Composite Preparation. Composites were prepared by solution mixing appropriate quantities of pristine SWNTs or **3** and the polymer in toluene at room temperature. The solutions were dried extensively at room temperature and subsequently annealed at 180 °C in a vacuum oven for ~24 h to remove any remaining solvent.

Melt Rheology. Samples for melt rheology were prepared by vacuum-molding ~1 g of the sample in a 25 mm die and pressed in a Carver press at 170 °C for 1 h using a maximum 1 ton load. Melt-state rheological measurements were performed on a Rheometric Scientific ARES rheometer with a torque transducer range of 0.2−2000 g_f cm using 25 mm diameter parallel plates with a sample thickness of 1−2 mm and a temperature range of 150−170 °C. Oscillatory strain ($\gamma(t)$) of the form

$$\gamma(t) = \gamma_0 \sin(\omega t) \tag{1}$$

where γ_0 is the strain amplitude (always less than 0.15 in the studies reported here and typically below 0.02) and ω is the frequency, is applied. The resulting time-dependent linear shear stress ($\sigma(t)$) is interpreted as

$$\sigma(t) = \gamma_0(G' \sin(\omega t) + G'' \cos(\omega t)) \tag{2}$$

where G' and G'' are the storage and loss modulus, respectively. All measurements in this study are linear (i.e., G' and G'' are independent of γ_0) and interpreted using eq 2.

Results and Discussion

The SWNTs utilized in the present experiments were produced by the HiPco process[16] and were purified according to literature methods.[17] The SWNTs were functionalized with 4-(10-hydroxy)decyl benzoate moieties (**3**) via in-situ generation of the corresponding aryl diazonium of **2**, according to a previously described method.[18] The reaction sequence is depicted in Figure 1, and detailed procedures are described in the Experimental Section. The functionalization results in significant changes in the spectroscopic properties of the SWNTs, as expected from previous work.[18−20] The solution phase absorption spectra of **3** and pristine SWNTs are shown in Figure 2. The absence of van Hove band structure in the spectrum of **3** is indicative of covalent modification. In the Raman spectrum of **3** (Figure 3b), the relative intensity of the D-band at ca. 1290 cm^{-1} is significantly increased compared to the spectrum of pristine SWNTs. This change is also indicative of covalent modification, as it reveals sp^3-hybridization or disorder within the nanotube framework. Previous work has demonstrated that the SWNTs are damaged by functionalization (although not quantifi-

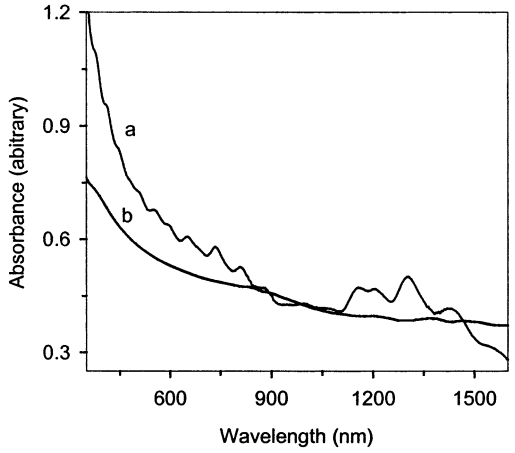

Figure 2. Absorption spectra in dimethylformamide: (a) pristine, unfunctionalized SWNTs; (b) material **3**.

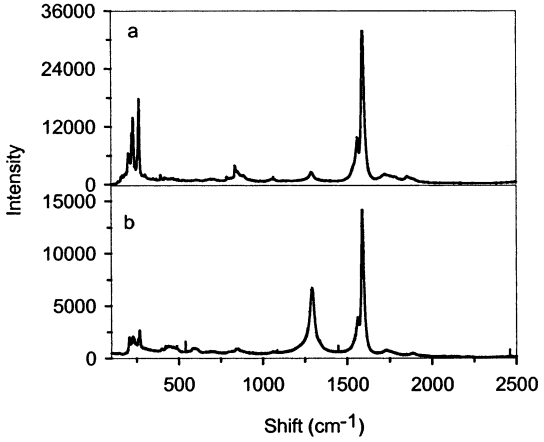

Figure 3. Raman scattering spectra from solid samples, with excitation at 782 nm: (a) pristine, unfunctionalized SWNTs; (b) material **3**.

able) and that the SWNT character is fully recovered following annealing to remove the functional moieties.[18,19]

Thermal gravimetric analysis (TGA) of **3** in an argon atmosphere (at 5 °C min^{-1}) revealed a significant mass loss on heating to 800 °C that is believed to represent loss of the functionalizing moieties from the SWNT surface. The residual mass after this treatment was 74%. On a weight basis, this corresponds to a stoichiometry of $C_{66}R$ where R is the functionalizing moiety. This degree of functionalization is sufficient to render the SWNTs more easily dispersed in organic media, although they are not truly soluble. Unfunctionalized HiPCO nanotubes and **3** (functionalized SWNTs) were solution mixed with a model polystyrene as described above, and the viscoelastic properties of the resulting composites were investigated.

The melt state linear dynamic oscillatory properties for the pristine polymer and a series of hybrids prepared with the unfunctionalized and functionalized (**3**) SWNTs were investigated. The data, using the smallest possible strain amplitudes, were collected over a narrow range of temperatures (160−180 °C) and superposed using the Boltzmann principle of time−temperature superpositioning to obtain viscoelastic mastercurves.[21] Horizontal (frequency) shift factors (a_T), with small vertical (modulus) shift factors (b_T) ($0.98 < b_T < 1.02$), were necessary to obtain complete superpositioning of the data sets. Moreover, these shift factors (over a very restricted

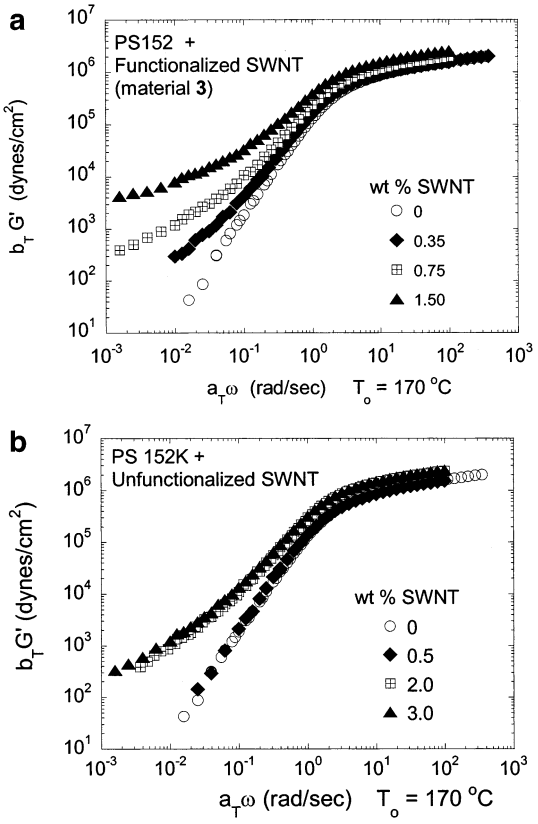

Figure 4. Master curves for the frequency dependence of the storage modulus (G') for the nanocomposites prepared with (a) **3** and (b) pristine unfunctionalized SWNTs. The data were shifted using the principle of time−temperature superpositioning and reduced to a reference temperature T_0 of 170 °C.

temperature range) were comparable for the polymer and the nanocomposites with both the functionalized and unfunctionalized SWNTs and consistent with prior values reported in the literature for polystyrene.[21]

Comparison of the influence of added unfunctionalized and functionalized SWNTs on the frequency dependence of the storage modulus (G') is demonstrated in Figure 4. We focus on the storage modulus (G') because the largest changes due to the reinforcement resulting from the added nanotubes are observed in this rheological property.[13] In particular, at low reduced frequencies ($a_T\omega$), the pure polymer behaves as a Newtonian liquid with the viscoelastic properties exhibiting liquidlike characteristics (i.e., $G' \propto \omega^2$, $G'' \propto \omega^1$, and $\eta^* \propto \omega^0$, where η^* is the complex viscosity and $G^*/\omega \equiv [(G')^2 + (G'')^2]^{1/2}/\omega$), while the nanocomposite with 1.5 wt % of the functionalized SWNTs exhibits pseudo-solid-like behavior (i.e., $G' \propto \omega^0$).[22]

For the functionalized SWNT-based nanocomposites, the low-frequency values of G', at any particular frequency, systematically increase with increasing SWNT loading and are accompanied by a progressive decrease in the low-frequency slope of log G' vs log($a_T\omega$). On the other hand, the hybrids prepared with up to 3 wt % of the unfunctionalized SWNTs do not demonstrate the same change in the frequency dependence of G'; in fact, the 0.75 wt % functionalized SWNT-based nanocomposite exhibits a higher low-frequency modulus (and weaker frequency dependence of G' at low frequencies) than the 3 wt % unfunctionalized SWNT-based composite as demonstrated in Figures 4 and 5. The high-frequency behavior, reflective of the dynamics on the

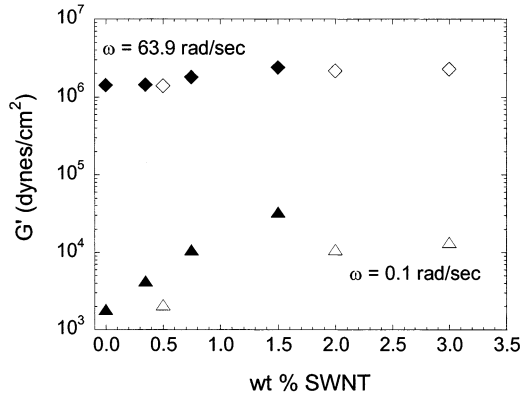

Figure 5. Comparison of storage modulus (G') values at two frequencies for the functionalized SWNT composites (filled symbols) and the unfunctionalized SWNT composites (open symbols). The diamonds correspond to a frequency (ω) of 63.9 rad/s at 170 °C and probe the dynamics in the entanglement regime of the polymer. The triangles represent data at ω = 0.1 rad/s and are representative of the data in the terminal flow zone of the polymer. The data for the functionalized and unfunctionalized SWNT composites are similar at high frequencies and considerably different at low frequencies.

length scale of an entanglement or smaller, on the other hand, demonstrates roughly the same composition dependence for the addition of the functionalized and unfunctionalized SWNTs as demonstrated in Figure 5. This high-frequency behavior suggests that the SWNTs do not significantly affect the dynamics of the PS chains on length scales comparable to the entanglement length.

Dramatic changes in the terminal zone (low frequency) behavior of the storage modulus, as observed for the functionalized SWNT−PS nanocomposites, have recently been demonstrated for macrocomposites of isotropic carbon black-filled elastomers,[10] polymer nanocomposites of highly anisotropic sheetlike layered silicates,[12,15,23] and multiwalled carbon nanotube composites[24] and has been attributed to the formation of a hydrodynamically percolated filler network structure. In addition to this frequency-independent behavior of G', the formation of a percolated filler network structure is accompanied by the development of a finite yield stress, which in the case of linear dynamic oscillatory flow behavior is manifested as a diverging η^* vs G^* plot as shown in Figure 6.[25] For the case of the functionalized SWNT-based hybrids, a divergence in the value of η^* is observed for the 1.5 wt % nanocomposite and is consistent with inferences of a percolated filler structure drawn from the frequency dependence of G'. In contrast, the unfunctionalized SWNT-based hybrids exhibit no such divergence even at 3 wt % SWNT loading, an observation consistent with a poorer dispersion of the nanotubes in this case.

The rheological data suggest that the extent of reinforcement and state of dispersion are considerably better for the functionalized SWNTs in PS as compared to the pristine SWNT in PS. Further, clear evidence for the formation of a percolated filler network structure is observed for the functionalized SWNTs at loadings as low as 1.5 wt % (or a volume fraction less than 1%), significantly lower than the ∼30 vol % required for the percolation of isotropic spheres in three dimensions.[26,27] Considerable lowering of the percolation threshold from that of isotropic noninteracting particles is observed due to either the anisotropic nature of the particles or the polymer-mediated interactions between particles.[10,12,15,23]

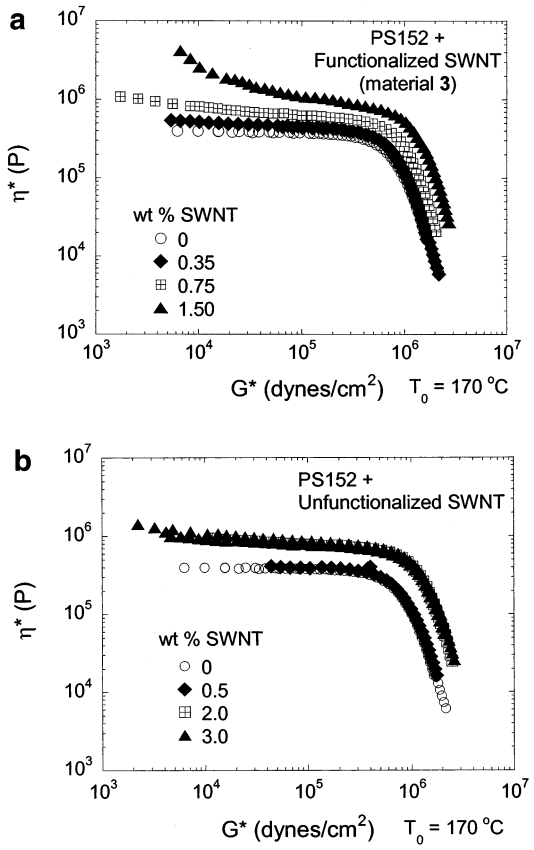

Figure 6. Dependence of the complex viscosity on the shear modulus for (a) functionalized and (b) pristine SWNT-based composites. The divergence in η^* at low G^* for the 1.5 wt % functionalized SWNT composite corresponds to the presence of a finite yield stress and the formation of a filler superstructure.

In the present case, we suggest that the organic modification of the SWNTs results in a better dispersion and demonstration of a higher anisotropy in these hybrids. In fact, for a system where percolation occurs at a loading of 1 vol %, it is anticipated that the effective anisotropy (in the absence of excluded-volume interactions) associated with the primary objects in the material is of the order of 100.[27] Inclusion of excluded-volume effects would probably lower the effective anisotropy.

However, the dispersion achieved for this combination of organic modification and polymer is probably not optimal. We do not anticipate any significantly favorable interactions between PS and the SWNTs, and this is verified by the poor dispersion of the pristine SWNTs in the PS matrix demonstrated here. Similarly, the organic surfactant-like tail of the functionalizing moiety in **3** does not have any exceedingly favorable interactions with the SWNT or the PS. The similarity of the high-frequency moduli for the functionalized and unfunctionalized SWNT-based composites (Figure 5) suggests that the reinforcement mechanism of the PS remained roughly unchanged with functionalization of the SWNT and further suggests that the interactions between the PS and the organic modifier are relatively weak.

The improved miscibility between PS and **3** could also emerge from the creation of the less repulsive PS/SWNT interactions at the expense of the more repulsive surfactant tail/SWNT interactions. This argument is similar to the detailed thermodynamic and experimentally based arguments used to assess the intercalation and

exfoliation of organically modified layered silicates by fairly nonpolar polymers such as polystyrene.[5,7] For these arguments to be valid, it is expected that the entropy of mixing and any entropy loss due to confinement of polymer chains near the SWNTs (or between SWNTs in the ropes) are negligibly small.[28] Further, it is assumed that in **3** the organic moieties at the surface of the SWNTs do not form an all-trans rigid structure. On the basis of prior studies of organically modified layered silicates,[29] and the 1 in 66 functionalization ratio in **3**, it is anticipated that in these sparsely functionalized systems the organic chains take on a liquidlike disordered state. This liquidlike structure results in significant SWNT/organic tail interactions in **3**, and the replacement of these highly unfavorable contacts by the slightly less unfavorable PS/SWNT interactions (resulting from the similarity of the structures and the slightly polar nature of PS)[30] results in the better dispersion. Thus, we anticipate that by carefully tailoring the interactions between the organic modification and the matrix polymer we can obtain significantly better dispersion and lowering of the percolation threshold than reported here.

Finally, the fact that we observe percolation at 1.5 wt % SWNTs is indeed quite remarkable. For the same polystyrene matrix, addition of a layered silicate (montmorillonite, organically modified with a double-tailed C18 cationic surfactant), considered as disks with thickness of ~1 nm and disk diameters of ~0.5 μm, results in a percolation threshold of ~5 wt % (2 vol %) layered silicates.[12] Non-Brownian disks and rods of similar aspect ratios are not expected to exhibit significantly different percolation thresholds. Thus, such a remarkable decrease in the percolation threshold for the SWNT-based composites suggests that the dispersion of the organically modified SWNTs is comparable to, if not significantly better than, that of the layered silicates in the same PS matrix.

Concluding Remarks

We have examined the linear viscoelastic properties of composites prepared with pristine SWNTs and organically modified SWNTs dispersed in a polystyrene matrix. The small strain oscillatory behavior is strongly influenced by the mesoscale dispersion of the added nanofillers, and the data reported here demonstrate the formation of a percolated filler network structure for the case of the organically modified SWNT with 1.5 wt % SWNT. In contrast, pristine SWNTs, when mixed with the same polystyrene matrix, do not exhibit the formation of a network superstructure for loadings as high as 3 wt % SWNT. In this context we observe that percolation at volume fractions of less than 0.01 implies that the effective anisotropy associated with the SWNTs in such composites is of the order of 100. We anticipate that the percolation threshold for the SWNT-based nanocomposites can be further lowered (and thus exploit the large aspect ratios afforded by these SWNTs) by either functionalizing the polymer or tailoring the organic modifier and thereby improve the interactions between the organic modifiers and the polymer matrix.

Acknowledgment. We thank Carbon Nanotechnologies, Inc., for the SWNTs. J.M.T. and J.L.B. thank funding from NASA (NASA-JSC-NCC 9-77, OSR 99091801) and NSF (NSR-DMR-0073046), C.A.M. thanks NASA for partial funding through the Graduate Research Fellowship, and R.K. thanks the Robert A. Welch Foundation for partial support of the research described here.

References and Notes

(1) Hadjiev, V. G.; Iliev, M. N.; Arepalli, S.; Nikolaev, P.; Files, B. S. *Appl. Phys. Lett.* **2001**, *78*, 3193−3195. Peigney, A.; Flahaut, E.; Laurent, C.; Chastel, F.; Rousset, A. *Chem. Phys. Lett.* **2002**, *352*, 20−25. Bower, C.; Rosen, R.; Zhou, O. *Appl. Phys. Lett.* **1999**, *74*, 3317. Haggenmueller, R.; Gommans, H. H.; Rinzler, A. G.; Fischer, J. E.; Winey, K. I. *Chem. Phys. Lett.* **2000**, *330*, 219.

(2) Bahr, J. L.; Tour, J. M. *J. Mater. Chem.* **2002**, *12*, 1952−1958.

(3) Kojima, Y.; Usuki, A.; Kawasumi, M.; Okada, A.; Kurauchi, T.; Kamigaito, O. *J. Polym. Sci., Part A: Polym. Chem.* **1993**, *31*, 983−986. Kojima, Y.; Usuki, A.; Kawasumi, M.; Okada, A.; Kurauchi, T.; Kamigaito, O.; Kaji, K. *J. Polym. Sci., Part B: Polym. Phys.* **1994**, *32*, 625−630. Kojima, Y.; Usuki, A.; Kawasumi, M.; Okada, A.; Kurauchi, T.; Kamigaito, O.; Kaji, K. *J. Polym. Sci., Part B: Polym. Phys.* **1995**, *33*, 1039−1045. Messersmith, P. B.; Giannelis, E. P. *J. Polym. Sci., Part A: Polym. Chem.* **1995**, *33*, 1047−1057. Messersmith, P. B.; Giannelis, E. P. *Chem. Mater.* **1993**, *5*, 1064−1066. Messersmith, P. B.; Giannelis, E. P. *Chem. Mater.* **1994**, *6*, 1719−1725. Usuki, A.; Kojima, Y.; Kawasumi, M.; Okada, A.; Fukushima, Y.; Kurauchi, T.; Kamigaito, O. *J. Mater. Res.* **1993**, *8*, 1174−1178. Usuki, A.; Koiwai, A.; Kojima, Y.; Kawasumi, M.; Okada, A.; Kurauchi, T.; Kamigaito, O. *J. Appl. Polym. Sci.* **1995**, *55*, 119−123. Giannelis, E. P. *Adv. Mater.* **1996**, *8*, 29.

(4) Giannelis, E. P.; Krishnamoorti, R.; Manias, E. *Adv. Polym. Sci.* **1999**, *138*, 107−147.

(5) Vaia, R. A.; Giannelis, E. P. *Macromolecules* **1997**, *30*, 8000−8008.

(6) Ginzburg, V. V.; Qiu, F.; Paniconi, M.; Peng, G.; Jasnow, D.; Balazs, A. C. *Phys. Rev. Lett.* **1999**, *82*, 4026−4029. Ginzburg, V. V.; Balazs, A. C. *Macromolecules* **1999**, *32*, 5681. Kuznetsov, V. D.; Balazs, C. A. *J. Chem. Phys.* **2000**, *112*, 4365−4375. Balazs, A. C.; Ginzburg, V. V.; Qiu, F.; Peng, G.; Jasnow, D. *J. Phys. Chem. B* **2000**, *104*, 3411−3422. Huh, J.; Balazs, A. C. *J. Chem. Phys.* **2000**, *113*, 2025−2031. Ginzburg, V. V.; Peng, G.; Qiu, F.; Jasnow, D.; Balazs, A. C. *Phys. Rev. E* **1999**, *60*, 4352−4359. Balazs, A. C.; Singh, C.; Zhulina, E. *Macromolecules* **1998**, *31*, 8370−8381. Lyatskaya, Y.; Balazs, A. C. *Macromolecules* **1998**, *31*, 6676−6680. Ginzburg, V. V.; Gibbons, C.; Qiu, F.; Peng, G.; Balazs, A. C. *Macromolecules* **2000**, *33*, 6140−6147. Balazs, A. C.; Singh, C.; Zhulina, E.; Lyatskaya, Y. *Acc. Chem. Res.* **1999**, *32*, 651−657.

(7) Vaia, R. A.; Giannelis, E. P. *Macromolecules* **1997**, *30*, 7990−7999.

(8) Vaia, R. A.; Jandt, K. D.; Kramer, E. J.; Giannelis, E. P. *Macromolecules* **1995**, *28*, 8080−8085.

(9) Yurekli, K.; Krishnamoorti, R. *Macromolecules* **2002**, *35*, 4075−4083. Watanabe, H.; Kotaka, T. *Polym. J.* **1982**, *14*, 739. Watanabe, H.; Kotaka, T. *Polym. J.* **1983**, *15*, 337−347. Watanabe, H.; Kotaka, T. *J. Rheol.* **1983**, *27*, 223. Watanabe, H.; Kotaka, T.; Hashimoto, T.; Shibayama, M.; Kawai, H. *J. Rheol.* **1982**, *26*, 153. Watanabe, H.; Sato, T.; Osaki, K.; Hamersky, M. W.; Chapman, B. R.; Lodge, T. P. *Macromolecules* **1998**, *31*, 3740−3742. Watanabe, H.; Sato, T.; Osaki, K.; Yao, M.-L. *Macromolecules* **1996**, *29*, 3890−3897. Watanabe, H.; Yao, M.-L.; Sato, T.; Osaki, K. *Macromolecules* **1997**, *30*, 5905−5912.

(10) Yurekli, K.; Krishnamoorti, R.; Tse, M. F.; McElrath, K. O.; Tsou, A. H.; Wang, H.-C. *J. Polym. Sci., Part B: Polym. Phys. Ed.* **2001**, *39*, 256−275.

(11) Newstein, M. C.; Wang, H.; Balsara, N. P.; Lefebvre, A. A.; Shnidman, Y.; Watanabe, H.; Osaki, K.; Shikata, T.; Niwa, H.; Morishima, Y. *J. Chem. Phys.* **1999**, *111*, 4827−4838.

(12) Krishnamoorti, R.; Yurekli, K. *Curr. Opin. Colloid Interface Sci.* **2001**, *6*, 464−470.

(13) Krishnamoorti, R.; Giannelis, E. P. *Macromolecules* **1997**, *30*, 4097−4102.

(14) Krishnamoorti, R.; Giannelis, E. P. *Langmuir* **2001**, *17*, 1448−1452. Krishnamoorti, R.; Ren, J.; Silva, A. S. *J. Chem. Phys.* **2001**, *114*, 4968−4973. Krishnamoorti, R.; Silva, A. S. In *Polymer-Clay Nanocomposites*; Pinnavaia, T. J., Beall, G. W., Eds.; John Wiley & Sons: New York, 2000; pp 315−343. Krishnamoorti, R.; Vaia, R. A.; Giannelis, E. P. *Chem. Mater.*

1996, *8*, 1728. Solomon, M. J.; Almusallam, A. S.; Seefeldt, K. F.; Somwangthanaroj, A.; Varadan, P. *Macromolecules* **2001**, *34*, 1864−1872.
(15) Ren, J.; Silva, A. S.; Krishnamoorti, R. *Macromolecules* **2000**, *33*, 3739−3746.
(16) Nikolaev, P.; Bronikowski, M. J.; Bradley, R. K.; Rohmund, F.; Colbert, D. T.; Smith, K. A.; Smalley, R. E. *Chem. Phys. Lett.* **1999**, *313*, 91−97.
(17) Chiang, I. W.; Brinson, B. E.; Huang, Y.; Willis, P. A.; Bronikowski, M. J.; Margrave, J. L.; Smalley, R. E.; Hauge, R. H. *J. Phys. Chem. B* **2001**, *105*, 8297−8301.
(18) Bahr, J. L.; Tour, J. M. *Chem. Mater.* **2001**, *13*, 3823−3824.
(19) Bahr, J. L.; Yang, J.; Kosynkin, D. V.; Bronikowski, M. J.; Smalley, R. E.; Tour, J. M. *J. Am. Chem. Soc.* **2001**, *123*, 6536−3542.
(20) Georgakilas, V.; Kordatos, K.; Prato, M.; Guldi, D. M.; Holzinger, M.; Hirsch, A. *J. Am. Chem. Soc.* **2002**, *124*, 760−761.
(21) Graessley, W. W. In *Physical Properties of Polymers*, 2nd ed.; American Chemical Society: Washington, DC, 1993.
(22) The data are considered to be pseudo-solidlike and not solidlike because true solidlike behavior would require the storage modulus G' to be independent of frequency and be considerably larger than the loss modulus G''. In the present case, the data indicate that while G' is reasonably independent of frequency, the values of G' and G'' remain fairly comparable.
(23) Ren, J.; Krishnamoorti, R. *Macromolecules*, **s**ubmitted for publication.
(24) Potschke, P.; Fornes, T. D.; Paul, D. R. *Polymer* **2002**, *43*, 3247−3255.
(25) Enikolopyan, N. S.; Fridman, M. L.; Stalnova, I. O.; Popov, V. L. *Adv. Polym. Sci.* **1990**, *96*, 1−67. Khan, S. A.; Prud'homme, R. K. *Rev. Chem. Eng.* **1987**, *4*, 205−270.
(26) Isichenko, M. B. *Rev. Mod. Phys.* **1992**, *64*, 961.
(27) Garboczi, E. J.; Snyder, K. A.; Douglas, J. F.; Thorpe, M. F. *Phys. Rev. E* **1995**, *52*, 819−828.
(28) Arnold, F. E., Jr.; Arnold, F. E. *Adv. Polym. Sci.* **1994**, *117*, 257.
(29) Vaia, R. A.; Teukolsky, R. K.; Giannelis, E. P. *Chem. Mater.* **1994**, *6*, 1017−1022. Vaia, R. A.; Ishii, H.; Giannelis, E. P. *Chem. Mater.* **1993**, *5*, 1694−1696.
(30) Van Oss, C. J.; Chaudhury, M. K.; Good, R. J. *Adv. Colloid Interface Sci.* **1987**, *28*, 35−64. Van Oss, C. J.; Chaudhury, M. K.; Good, R. J. *Sep. Sci. Technol.* **1989**, *24*, 15−30.

MA020890Y